Development of alkoxy styrylchromone derivatives for imaging of cerebral amyloid-*β* plaques with SPECT

Takeshi Fuchigami[a*], Ayaka Ogawa[a], Yuki Yamashita[a], Mamoru Haratake[a,b], Hiroyuki Watanabe[c], Masahiro Ono[c], Masao Kawasaki[a], Sakura Yoshida[a], Morio Nakayama[a*]

[a] Department of Hygienic Chemistry, Graduate School of Biomedical Sciences, Nagasaki University, 1-14 Bunkyo-machi, Nagasaki 852-8521, Japan

[b] Faculty of Pharmaceutical Sciences, Sojo University, 4-22-1 Ikeda, Kumamoto 860-0082, Japan

[c] Graduate School of Pharmaceutical Sciences, Kyoto University, 46-29 Yoshida Shimoadachi-cho, Sakyo-ku, Kyoto 606-8501, Japan.

*corresponding author:

Takeshi Fuchigami,

Graduate School of Biomedical Sciences, Nagasaki University, 1-14 Bunkyo-machi, Nagasaki 852-8521, Japan.

Tel.: +81-95-819-2443;

Fax: +81-95-819-2443;

E-mail: t-fuchi@nagasaki-u.ac.jp

Morio Nakayama,

Graduate School of Biomedical Sciences, Nagasaki University, 1-14 Bunkyo-machi, Nagasaki 852-8521, Japan.

Tel.: +81-95-819-2441;

Fax: +81-95-819-2441;

E-mail: morio@nagasaki-u.ac.jp

Abstract

We report here the development of radioiodinated styrylchromone derivatives with alkoxy groups as single photon emission computed tomography (SPECT) imaging probes for cerebral amyloid-β (Aβ) plaques. Among the derivatives, the methoxy derivative **14** and the dimethoxy derivative **15** displayed relatively high affinity for the Aβ(1–42) aggregates with Ki values of 22 and 46 nM, respectively. Fluorescent imaging demonstrated that **14** and **15** clearly labeled thioflavin-S positive Aβ plaques in the brain sections of *Tg2576* transgenic mice. In the *in vivo* studies, [^{125}I]**14** and [^{125}I]**15** showed high initial brain uptake expressed as

the percentage of the injected dose per gram (2.25% and 2.49% ID/g at 2 min, respectively) with favorable clearance (0.12% and 0.20% ID/g at 180 min, respectively) from the brain tissue of normal mice. Furthermore, *in vitro* autoradiography confirmed that [^{125}I]**15** binds thioflavin-S positive regions in *Tg2576* mouse brain sections. The derivative **15** may be a potential scaffold for the development of *in vivo* imaging probes targeting A*β* plaques in the brain. In particular, further structural modifications are required to improve the compounds binding affinity for A*β*.

Key words: Alzheimer's disease, amyloid-*β* plaque, styrylchromone, single photon emission computed tomography (SPECT).

Alzheimer's disease (AD), which is the most common cause of dementia in the elderly, is characterized by the progressive decline of cognition including learning and memory[1]. It is estimated that the number of patients with AD will increase to over 100 million by the year 2050 and, for this reason, effective therapies need to be developed to prevent the collapse ofglobal health-care systems[2]. A*β* plaques have been detected in patients prior to the appearance of the clinical symptoms of AD. This implies that the detection and early initiation of treatment targeting A*β* deposits could be an effective therapeutic option to improve the symptoms of AD patients in the early disease stage[2,3]. Nuclear medicine imaging techniques

have been accepted as useful tools for the early detection of cerebral Aβ plaque deposits[4].

Numerous studies have reported the development of positron emission tomography (PET) and

SPECT imaging probes of Aβ plaques in the living brain[5-7]. In particular, ^{18}F-flutemetamol,

[18]F-florbetapir and ^{18}F-florbetaben have demonstrated highly correlated brain distribution

patterns with post-mortem existence of Aβ plaques. Recently, these PET tracers were

approved by the US Food and Drug Administration (FDA) for the specific detection of Aβ

plaques inclinical practice[8-10]. In contrast, there are currently no effective SPECT probes for

detecting Aβ plaques despite their convenience and widespread utilization. SPECT is widely

available in most hospitals, and is generally less expensive, as compared to PET[11,12].

Accordingly, the development of clinically useful SPECT imaging probes for Aβ can facilitate

and encourage the initial diagnosis of AD in elderly people. Previously, we have developed

flavonoid derivatives such as flavones, chalcones, aurones, and styrylchromones as

prospective Aβ imaging probes, although clinically available compounds have not yet been

developed[13-22]. We found that radioiodinated styrylchromones (SCs) with amino groups (NH$_2$,

NHMe, and NMe$_2$) bind to Aβ aggregates with high binding affinities. However, their initial

uptake and washout from normal mice brain tissue were inadequate for *in vivo* imaging[22].

Therefore, we hypothesized that the structural modification of SCs may improve the *in vivo*

brain distribution and thereby, provide useful Aβ imaging agents. Previously, we reported that

radioiodinated flavonoids such as flavone, chalcone, and aurone derivatives with alkoxy

groups at the *p*-position of the phenyl ring showed good initial brain uptake and washout from the normal brain without crucial decline in binding affinity for $A\beta$[13,19,21]. Therefore, we considered that the introduction of alkoxy groups to the structure of SCs could improve their *in vivo* brain distribution. For this reason, we designed new radioiodinated SCs derivatives, which have alkoxy groups introduced into the 2-phenyl ring of the original structure. We envisaged that this structural modification would enable their application in SPECT diagnosis.

The synthesis of the alkoxy SC derivatives is presented in Scheme 1. *O*-acylation of the 5'-bromo-2'-hydroxyacetophenone with the appropriate cinnamoyl chlorides provided phenyl cinnamates **1-3**. The Baker–Venkataraman rearrangement of the phenyl cinnamates using KOH gave the corresponding 1,3-diketones **4-6**. The treatment of these 1,3-diketones with a mixture of H_2SO_4 and AcOH led to their cyclodehydration yielding (*E*)-2-styrylchromones **7-9**. These styrylchromones were converted to tributyltin derivatives **10-12** using a bromo-to-tributyltin exchange reaction catalyzed by Pd(0). The resulting tributyltin derivatives were reacted with iodine in $CHCl_3$ to form the target iodo derivatives **13-15**. Methoxy derivative **14** was converted to phenol derivative **16** by demethylation with BBr_3 in CH_2Cl_2. Alkylation of **16** with ethylene chlorohydrin, ethylene glycol mono-2-chloroethyl ether, or 2-[2-(2-chloroethoxy)ethoxy]ethanolusing potassium carbonate resulted in oligoethyleneoxy derivatives **17**, **18**, and **19**, respectively.

In vitro binding experiments to evaluate, the binding affinity of the SC derivatives for

Aβ were performed. We used suspensions of Aβ(1–42) aggregates with ^{125}I-labeled 4-dimethylamino-4'-iodo-styrylchromone (**20**), which showed high binding affinity for Aβ aggregates (K_d = 8.7 nM) in our previous studies[22]. The inhibition constant (K_i) values of the SCs for the Aβ aggregates ranged from 21.9 to 553nM (Table 1). Derivative **13**, which contained an unsubstituted 2-phenyl ring, displayed weak affinity for Aβ aggregates (K_i = 198 nM). In contrast, methoxy derivative **14** (K_i = 21 nM) showed a 9-fold improvement in binding affinity versus **13**, displaying comparable affinity to dimethylamino derivative **20** (K_i = 22 nM). Accordingly, the presence of a methoxy group at R_1 may have a crucial role in binding interactions with Aβ aggregates. Dimethoxy derivative **15** had a reasonable binding affinity (K_i = 46 nM), suggesting that the introduction of a methoxy group at the R_2 position can retain binding affinity. However, introduction of a hydroxyl group at the R_1 position did not improve the binding affinity. Indeed, hydroxyl derivative **16** displayed a negligible Aβ binding affinity (K_i = 121 nM). The oligoethyleneoxy derivatives **17-19** exhibited reduced binding affinities (K_i = 415-553 nM), which were over 20-fold lower than **14**. In our previous study, the introduction of oligoethyleneoxy groups to the phenyl ring of radioiodinated aurones did not considerably alter Aβ aggregate binding[21]. In this study, we observed the opposite effect, in that the presence of oligoethyleneoxy groups on the 2-phenyl ring of the SCs clearly had a deleterious effect on Aβ aggregate binding affinity. These facts suggest that SCs and aurones may exhibit different binding interactions with Aβ aggregates, although the

mechanisms remain largely unclear.

Based on the *in vitro* results, we selected **14** and **15** for further biological evaluation. Fluorescence imaging experiments with the SCs were performed using brain slices from a transgenic mouse (*Tg2576*) model of Aβ deposition. A number of fluorescence spots denoting derivatives **14** and **15** were observed in the mouse brain slices (Figs. 2A and B). The labeling patterns of these compounds corresponded to the fluorescence signals obtained with thioflavin-S staining (Figs. 2C and D). In contrast, there was no significant fluorescence for **14** and **15** in the brain slices from wild-type mice (Figs. 2E and F). There was no marked autofluorescence detected in any brain slices (data not shown). These results indicate that **14** and **15** have specific binding potential to Aβ plaques in the mouse brain.

For the biodistribution study and *in vitro* autoradiography, ^{125}I-labeled SC derivatives ($[^{125}I]$**14**, $[^{125}I]$**15**) were synthesized by an iododestannylation reaction of tributyltin derivatives (**11** and **12**) with hydrogen peroxide as an oxidant (Scheme 2). Using HPLC systems, the radioligands were purified, and the radiochemical qualities of these ligands were analyzed by co-injection of non-radioactive compounds. The radioiodinated products were obtained in radiochemical yields of 40-75% with a radiochemical purity of >95%. Clinically available SPECT imaging probes for the Aβ plaque should show a high initial brain uptake and rapid clearance from non-target regions in the brain. Therefore, biodistribution studies of $[^{125}I]$**14** and $[^{125}I]$**15** were conducted in normal mice and expressed as % of injected dose per

gram (%ID/g) (Table 2). The compounds $[^{125}I]$**14** and $[^{125}I]$**15** exhibited a high initial brain

uptake (2.3% and 2.5% ID/g at 2 min, respectively) and a favorable brain clearance (0.1%

and 0.2% ID/g at 180 min, respectively). The $brain_{2min}/brain_{60min}$ ratio of ^{18}F has been used as

an index of brain washout[23,24]. The $brain_{2min}/brain_{60min}$ ratio of clinically used $[^{18}F]$Florbetapir

($[^{18}F]$AV-45) and $[^{18}F]$Florbetaben ($[^{18}F]$BAY94-917218) was reported to be 3.8[23] and 4.8[25],

respectively. Since the $brain_{2min}/brain_{60min}$ ratio of $[^{125}I]$**14** and $[^{125}I]$**15** was calculated to be

4.5 and 3.3, respectively, the washout index of these $[^{125}I]$SC derivatives seems to be

comparable to the aforementioned PET probes. Additionally, because the half-life of

radioactive iodine ^{123}I, used for SPECT, is much longer than that of ^{18}F (13.2 h vs 110 min),

the $brain_{2min}/brain_{180min}$ ratio can be used as another index of brain washout in this study. The

$brain_{2min}/brain_{180min}$ ratios of $[^{125}I]$**14** and $[^{125}I]$**15** were 18.8 and 12.5, respectively, indicating

that these two ^{125}I-labeled SC derivatives have promising *in vivo* pharmacokinetics.

Furthermore, the collective *in vivo* results suggested that the washout of $[^{125}I]$**14** from the

normal brain tissue was faster than that of $[^{125}I]$**15**. Both $[^{125}I]$**14** and $[^{125}I]$**15** demonstrated

increased radioactivity in the stomach over time, and peaked at 5.0% and 5.2% ID/g at 60

min, respectively, suggesting that these SCs were gradually deionidated *in vivo*. Since brain

uptake of these tracers rapidly declined with time, it is unlikely that the metabolites could

easily penetrate the blood brain barrier. Consistent with our previous study[22], relatively low

initial brain uptake and high brain retention of the dimethylamino derivative $[^{125}I]$**20** (1.20%

ID/g at 2 min and 0.38% ID/g at 180 min) was observed, compared with the methoxy derivatives. It is reported that radiotracers with a low molecular weight (<500 Da) and a moderate lipophilicity (log$D_{7.4}$ values, 2.0–3.5) show optimal passive brain entry *in vivo*[26,27]. Although the molecular weights of the ^{125}I-labeled compounds in this study are all within the specified range (Table 2), the most lipophilic [125I]**20** showed a relatively low blood-brain barrier permeability. Taken together, these results indicate that the substitution of a dimethylamino group with methoxy groups at the 2-phenyl ring position of the SCs structure improves its brain distribution for *in vivo* imaging.

To further characterize [125I]**14** and [125I]**15** as possible imaging probes for specifically targeting Aβ plaques, *in vitro* autoradiography was performed using brain sections from the *Tg2576* mice. Although some [125I]**14** spots in the brain slices corresponded to thioflavin-S stained regions, the overall [125I]**14** image was inconsistent with the existence of Aβ plaques (Fig. 3A and 3C). In contrast, clear [125I]**15** autoradiographic images were observed in the thioflavin-S positive regions (Fig. 3B and 3D). The discrepancy between the fluorescence and autoradiographic images of these SC derivatives could have been caused by the different concentration of the compounds. The concentration of the SCs was 100 μM for the fluorescence staining while only 0.3 nM of 125I labeled SCs was used in the autoradiography studies. It is unclear why only the [125I]**15** displayed a clear autoradiograph for Aβ plaques, despite the fact that derivative **15** possesses a lower binding affinity for the Aβ aggregates

than **14** (Table 1). Several factors may have contributed to these results, including the selectivity for Aβ plaques over other brain components, degree of nonspecific binding, and conformation differences between the Aβ aggregates and Aβ plaques in the brain of *Tg2576* mice. Regardless, the [^{125}I]**15** may be a potential lead compound for the development of *in vivo* imaging probes for Aβ plaques in the brain. Further structural modification of the SC derivatives can provide promising Aβ imaging probes.

In conclusion, we demonstrated that radioiodinated styrylchromone derivatives with methoxy groups had preferable pharmacokinetics for *in vivo* imaging without significant reduction in binding affinity for the Aβ aggregates. In particular, both fluorescent imaging and autoradiography showed that the dimethoxy derivative [^{125}I]**15** labeled the thioflavin-S positive Aβ plaques in sections of the *Tg2576* mouse brain. Further structural modifications based on derivative **15** may facilitate the development of clinically useful Aβ imaging probes.

Acknowledgments

References

1. Querfurth, H. W.; LaFerla, F. M. *N. Engl. J. Med.* **2010**, 362, 329.

2. Karran, E.; Mercken, M.; De Strooper, B. *Nat. Rev. Drug. Discov.* **2011**, 10, 698.

3. Selkoe, D. *J.Physiol. Rev.* **2001**, 81, 741.

4. Shokouhi, S.; Claassen, D.; Riddle, W. *J.Alzheimers. Dis. Parkinsonism.* **2014**, 4, 143.

5. Kung, H. F.; Choi, S. R.; Qu, W.; Zhang, W.; Skovronsky, D.*J. Med. Chem.* **2010**,53, 933.

6. Ono, M.; Saji, H. *J. Pharmacol. Sci.* **2012**, 118, 338.

7. Yang, Y.; Cui, M.*Eur. J. Med. Chem.* **2014**, 87, 703.

8. Vandenberghe, R.; Adamczuk, K.; Dupont, P.; Laere, K. V.; Chételat, G. *Neuroimage Clin.* **2013**, 2, 497.

9. Williams, S.C.P. *Nat. Med.* **2013**, 19, 1551.

10. Senda, M.; Sasaki, M.; Yamane, T.; Shimizu, K.; Patt, M.; Barthel, H.; Sattler, B.; Nagasawa, T.; Schultze-Mosgau, M.; Aitoku, Y.; Dinkelborg, L.; Sabri, O. *Eur. J. Nucl. Med. Mol. Imaging.* **2014**, 42, 89.

11. Mariani, G.; Bruselli, L.; Kuwert, T.; Kim, E. E.; Flotats, A.; Israel, O.; Dondi, M.; Watanabe, N. *Eur. J. Nucl. Med. Mol. Imaging.* **2010**, 37, 1959.

12. Adak, S.; Bhalla, R.; Raj, K. K. V.; Mandal, S.; Pickett, R.; Luthra, S. K. *Radiochim. Acta.* **2012**, 100, 95.

13. Ono, M.; Yoshida, N.; Ishibashi, K.; Haratake, M.; Arano, Y.; Mori, H.; Nakayama, M. *J. Med. Chem.* **2005**, 48, 7253.
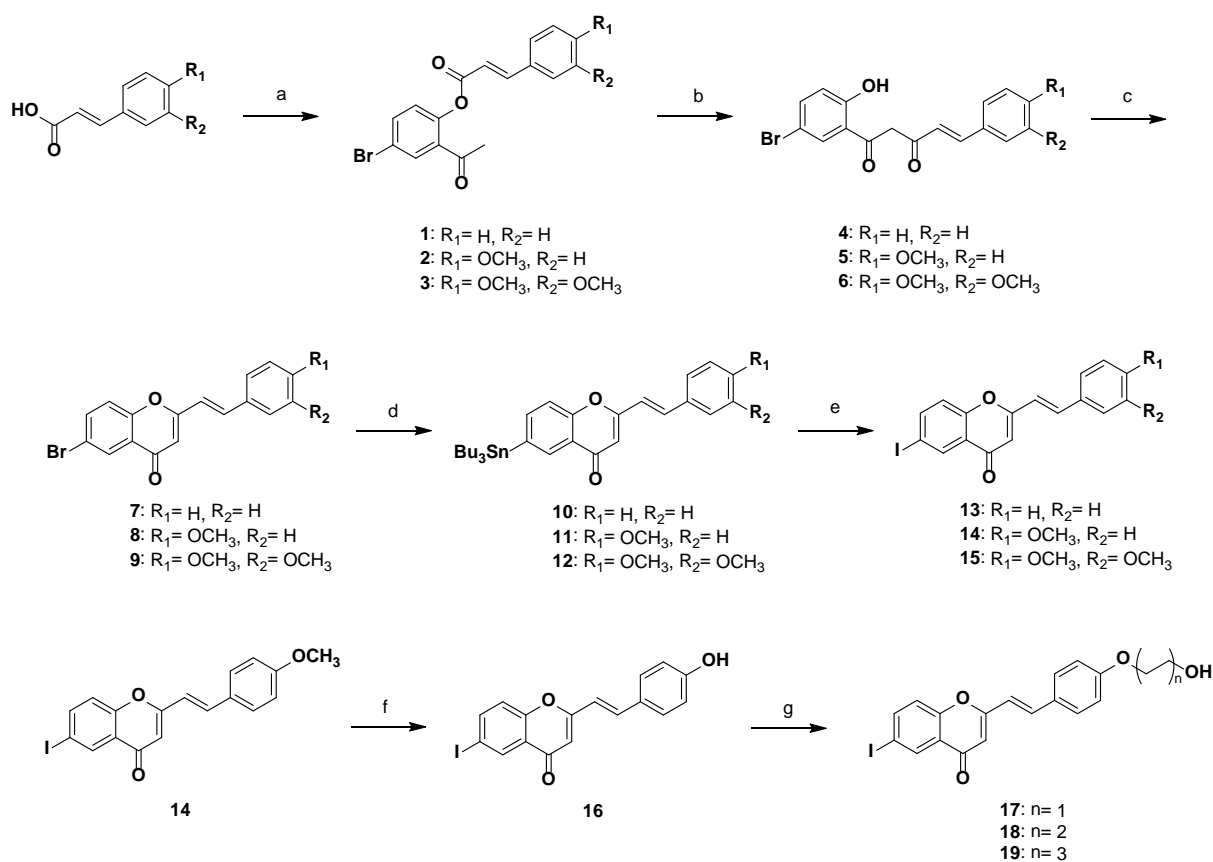
14. Ono, M.; Watanabe, R.; Kawashima, H.; Kawai, T.; Watanabe, H.; Haratake, M.; Saji, H.; Nakayama, M. *Bioorg. Med. Chem.* **2009**, 17, 2069.

15. Ono, M.; Hori, M.; Haratake, M.; Tomiyama, T.; Mori, H.; Nakayama, M. *Bioorg. Med. Chem.* **2007**, 15 6388.

16. Ono, M.; Haratake, M.; Mori, H.; Nakayama, M. *Bioorg. Med. Chem.* **2007**, 15, 6802.

17. Ono, M.; Watanabe, R.; Kawashima, H.; Cheng, Y.; Kimura, H.; Watanabe, H.; Haratake, M.; Saji, H.; Nakayama, M. *J. Med. Chem.* **2009**, 52, 6394.

18. Ono, M.; Ikeoka, R.; Watanabe, H.; Kimura, H.; Fuchigami, T.; Haratake, M.; Saji, H.; Nakayama, M. *ACS Chem. Neurosci.* **2010**, 1, 598.

19. Fuchigami, T.; Yamashita, Y.; Haratake, M.; Ono, M.; Yoshida, S.; Nakayama, M. *Bioorg. Med. Chem.* **2014**, 22, 2622.

20. Ono, M.; Maya, Y.; Haratake, M.; Ito, K.; Mori, H.; Nakayama, M. *Biochem. Biophys. Res. Commun.* **2007**, 361, 116.

21. Maya, Y.; Ono, M.; Watanabe, H.; Haratake, M.; Saji, H.; Nakayama, M. *Bioconjug. Chem.* **2009**, 20, 95.

22. Ono, M.; Maya, Y.; Haratake, M.; Nakayama, M. *Bioorg. Med. Chem.* **2007**, 15, 444.

23. Zhang, W.; Oya, S.; Kung, M. P.; Hou, C.; Maier, D. L.; Kung, H. F. *Nucl. Med. Biol.* **2005**, 32, 799.

24. Ono, M.; Cheng, Y.; Kimura, H.; Cui, M.; Kagawa, S.; Nishii, R.; Saji, H. *J. Med. Chem.*
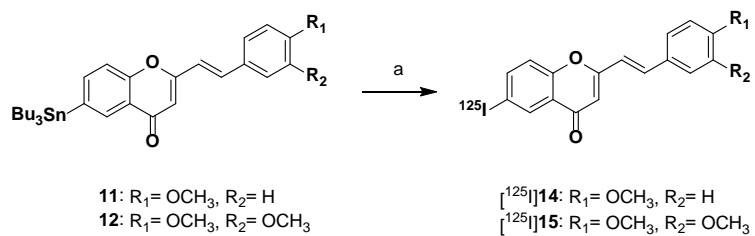
2011, 54, 2971.

25. Zhang, W.; Kung, M. P.; Oya, S.; Hou, C.; Kung, H. F. *Nucl. Med. Biol.* **2007**, 34, 89.

26. Pike, V. W. *Trends. Pharmacol. Sci.* **2009**, 30, 431.

27. Waterhouse, R. N. *Mol. Imaging. Biol.* **2003**, 5, 376.

Scheme 1. Synthesis of styrylchromone derivatives.

1: R$_1$= H, R$_2$= H
2: R$_1$= OCH$_3$, R$_2$= H
3: R$_1$= OCH$_3$, R$_2$= OCH$_3$

4: R$_1$= H, R$_2$= H
5: R$_1$= OCH$_3$, R$_2$= H
6: R$_1$= OCH$_3$, R$_2$= OCH$_3$

7: R$_1$= H, R$_2$= H
8: R$_1$= OCH$_3$, R$_2$= H
9: R$_1$= OCH$_3$, R$_2$= OCH$_3$

10: R$_1$= H, R$_2$= H
11: R$_1$= OCH$_3$, R$_2$= H
12: R$_1$= OCH$_3$, R$_2$= OCH$_3$

13: R$_1$= H, R$_2$= H
14: R$_1$= OCH$_3$, R$_2$= H
15: R$_1$= OCH$_3$, R$_2$= OCH$_3$

14

16

17: n= 1
18: n= 2
19: n= 3

Reagents and conditions: (a) 1) SOCl$_2$, DMF, reflux 1 h, 2) 5'-Bromo-2'-hydroxyacetophenone, pyridine, reflux, 3 h; (b) pyridine, KOH, reflux, 1h; (c) H$_2$SO$_4$, AcOH, reflux, 1 h then r.t., 1h; (d) (SnBu$_3$)$_2$, Pd(PPh$_3$)$_4$, Et$_3$N, dioxane, reflux, 7 h, (e) I$_2$, CHCl$_3$, r.t., 30 min (f) CH$_2$Cl$_2$, BBr$_3$, r.t., 24 h; (g) H(OCH$_2$CH$_2$)$_n$Cl, K$_2$CO$_3$, DMF.

Scheme 2. Radiosynthesis of ^{125}I-labeled styrylchromone derivatives.

11: R$_1$= OCH$_3$, R$_2$= H
12: R$_1$= OCH$_3$, R$_2$= OCH$_3$

[^{125}I]**14**: R$_1$= OCH$_3$, R$_2$= H
[^{125}I]**15**: R$_1$= OCH$_3$, R$_2$= OCH$_3$

Reagents and conditions: (a) [^{125}I]NaI, H$_2$O$_2$, HCl, EtOH, 3 min.

Table 1. Inhibition constant (K_i) for Aβ (1-42) aggregates and log P values of styrylchromone

derivatives.
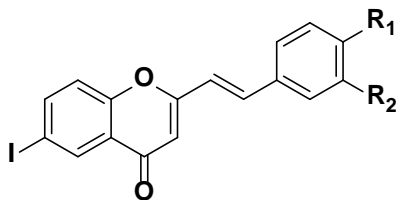
13: R_1= H, R_2= H
14: R_1= OMe, R_2= H
15: R_1= OMe, R_2= OMe
16: R_1= OH, R_2= H
17: R_1= OCH$_2$CH$_2$OH, R_2= H
18: R_1= (OCH$_2$CH$_2$)$_2$OH, R_2= H
19: R_1= (OCH$_2$CH$_2$)$_3$OH, R_2= H
20: R_1= N(CH$_3$)$_2$, R_2= H

Compounds	K_i[a] (nM)			Mw	log P[b]
13	198	$\pm$	48.0	374.1	−
14	21.9	$\pm$	5.10	404.2	2.15
15	45.5	$\pm$	10.7	434.2	2.14
16	121	$\pm$	20.8	390.2	1.87
17	446	$\pm$	100	434.2	−
18	415		64.5	478.3	−
19	553		135	522.3	−
20	21.8	$\pm$	3.35	417.3	2.65[c]

[a] Inhibition constant of styrylchromone derivatives were determined using [^{125}I]**20** as the ligand in Aβ aggregates. Each value (mean ± SEM) was determined by 3-6 independent experiments.

[b] The partition coefficient between *n*-octanol and sodium phosphate buffer at pH 7.4 was determined by a conventional flask shaking method (n = 3).

[c] The log *P* values have been reported in our previous studies[22].

Table 2. Biodistribution of radioactivity after *i.v.* injection of ^{125}I labeled styrylchromone derivatives in normal mice.

Organ	Time after injection (min)				
	2	30	60	120	180
			$[^{125}I]$**14**		
Blood	2.22 (0.31)	0.76 (0.09)	0.56 (0.13)	0.36 (0.08)	0.29 (0.04)
Liver	20.90 (3.32)	14.72 (3.73)	9.10 (2.58)	6.53 (3.63)	3.38 (0.59)
Kidney	10.06 (1.94)	4.50 (1.55)	2.20 (0.41)	1.28 (0.40)	0.85 (0.12)
Intestine	1.70 (0.67)	10.41 (3.60)	18.57 (7.07)	22.64 (6.14)	18.82 (3.81)
Spleen	3.81 (1.11)	1.19 (0.20)	0.82 (0.17)	0.70 (0.26)	0.55 (0.32)
Lung	6.12 (1.61)	1.77 (0.33)	1.17 (0.28)	0.78 (0.18)	0.60 (0.19)
Stomach	0.96 (0.26)	1.22 (0.88)	2.58 (2.09)	5.03 (4.15)	4.19 (1.37)
Pancreas	5.26 (0.84)	1.44 (0.22)	1.06 (0.44)	0.82 (0.74)	0.68 (0.72)
Heart	5.50 (1.08)	1.09 (0.08)	0.67 (0.15)	0.37 (0.10)	0.26 (0.08)
Brain	2.25 (0.38)	1.00 (0.12)	0.56 (0.11)	0.23 (0.06)	0.12 (0.02)
			$[^{125}I]$**15**		
Blood	3.42 (0.32)	1.25 (0.16)	0.74 (0.10)	0.61 (0.14)	0.33 (0.05)
Liver	15.07 (1.39)	7.42 (1.46)	4.98 (1.39)	3.50 (0.82)	4.26 (0.80)

|					
Kidney	12.28 (1.43)	4.74 (0.70)	2.37 (0.33)	1.51 (0.18)	1.09 (0.20)
Intestine	1.71 (0.47)	12.19 (4.91)	15.93 (8.64)	27.37 (4.85)	23.16 (3.95)
Spleen	4.86 (0.69)	1.62 (0.31)	1.04 (0.16)	0.80 (0.49)	1.33 (1.19)
Lung	7.00 (0.99)	2.31 (0.31)	1.46 (0.18)	0.95 (0.11)	1.68 (2.48)
Stomach	1.39 (0.18)	2.75 (2.17)	1.77 (0.53)	5.15 (3.29)	3.67 (2.82)
Pancreas	7.17 (1.62)	2.95 (0.90)	1.13 (0.17)	0.76 (0.34)	0.42 (0.20)
Heart	6.96 (0.93)	1.68 (0.23)	0.96 (0.13)	0.52 (0.08)	0.32 (0.08)
Brain	2.49 (0.39)	1.39 (0.16)	0.76 (0.12)	0.36 (0.05)	0.20 (0.12)

$[^{125}I]$**20**

Blood	2.24 (0.43)	1.20 (0.17)	1.02 (0.16)	1.07 (0.19)	1.09 (0.29)
Liver	12.3 (2.65)	8.36 (2.01)	5.84 (1.18)	7.46 (2.61)	4.36 (1.29)
Kidney	8.68 (2.05)	3.36 (1.25)	1.59 (0.66)	1.35 (0.55)	1.37 (0.41)
Intestine	1.20 (0.48)	11.83 (2.26)	9.90 (5.68)	13.43 (5.52)	10.03 (2.58)
Spleen	3.88 (1.94)	2.65 (0.45)	1.82 (0.45)	2.01 (0.89)	2.04 (0.29)
Lung	8.83 (2.51)	3.85 (0.69)	2.54 (0.82)	2.27 (0.55)	1.96 (0.89)
Stomach	1.01 (0.31)	1.88 (0.79)	1.79 (0.66)	3.15 (1.46)	3.38 (2.68)
Pancreas	3.37 (0.59)	1.44 (0.58)	0.84 (0.14)	0.81 (0.31)	0.59 (0.21)
Heart	5.51 (1.33)	1.26 (0.31)	0.66 (0.13)	0.63 (0.14)	0.64 (0.17)

| Brain | 1.20 (0.23) | 1.13 (0.21) | 0.62 (0.10) | 0.44 (0.11) | 0.38 (0.11) |

Each value represents mean (SD) for 5 or 6 mice at each interval.
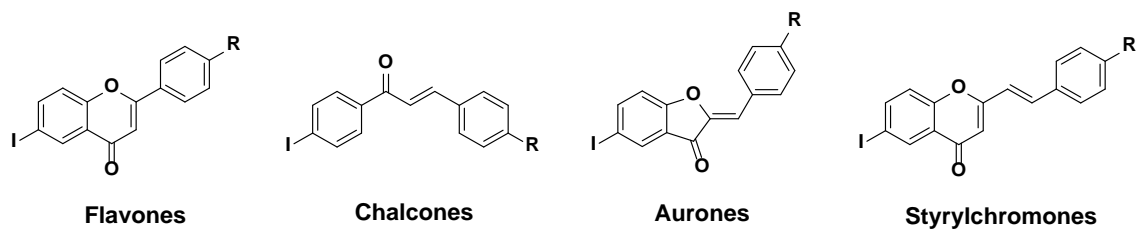
Figure 1. Chemical structures of flavonoid derivatives reported as Aβ imaging probes.
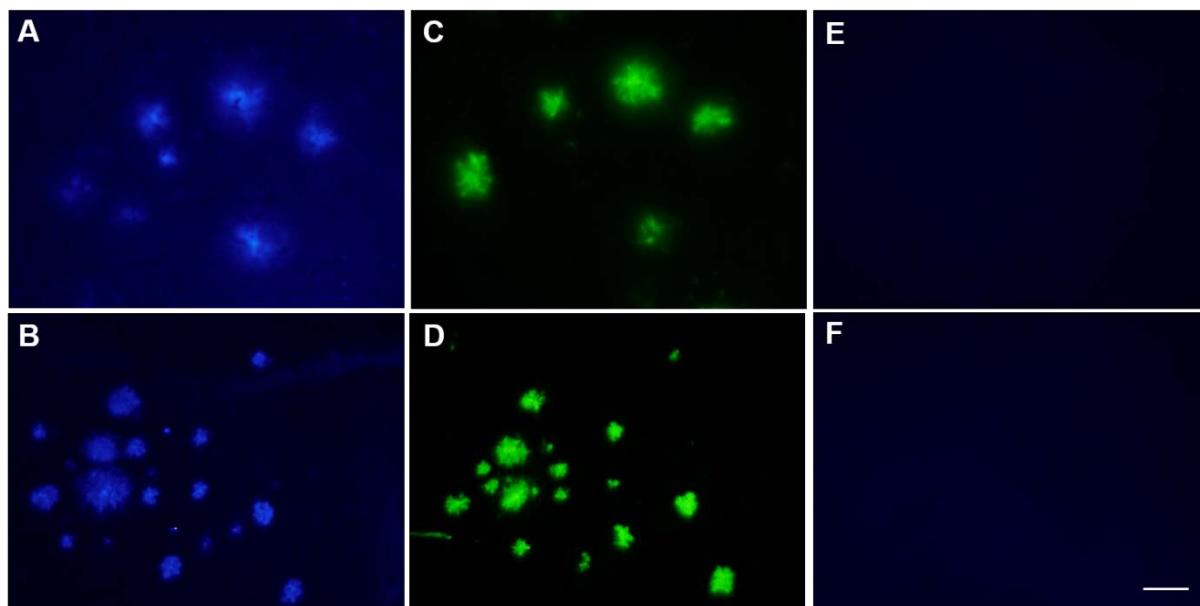
Figure 2. Neuropathological staining of styrylchromone derivatives **14** (A) and **15** (B) in 10

μm sections of *Tg2576* mice brain. Labeled plaques were confirmed by staining of the

adjacent sections with thioflavin-S (C and D). Fluorescence images of **14** (E) and **15** (F) in the

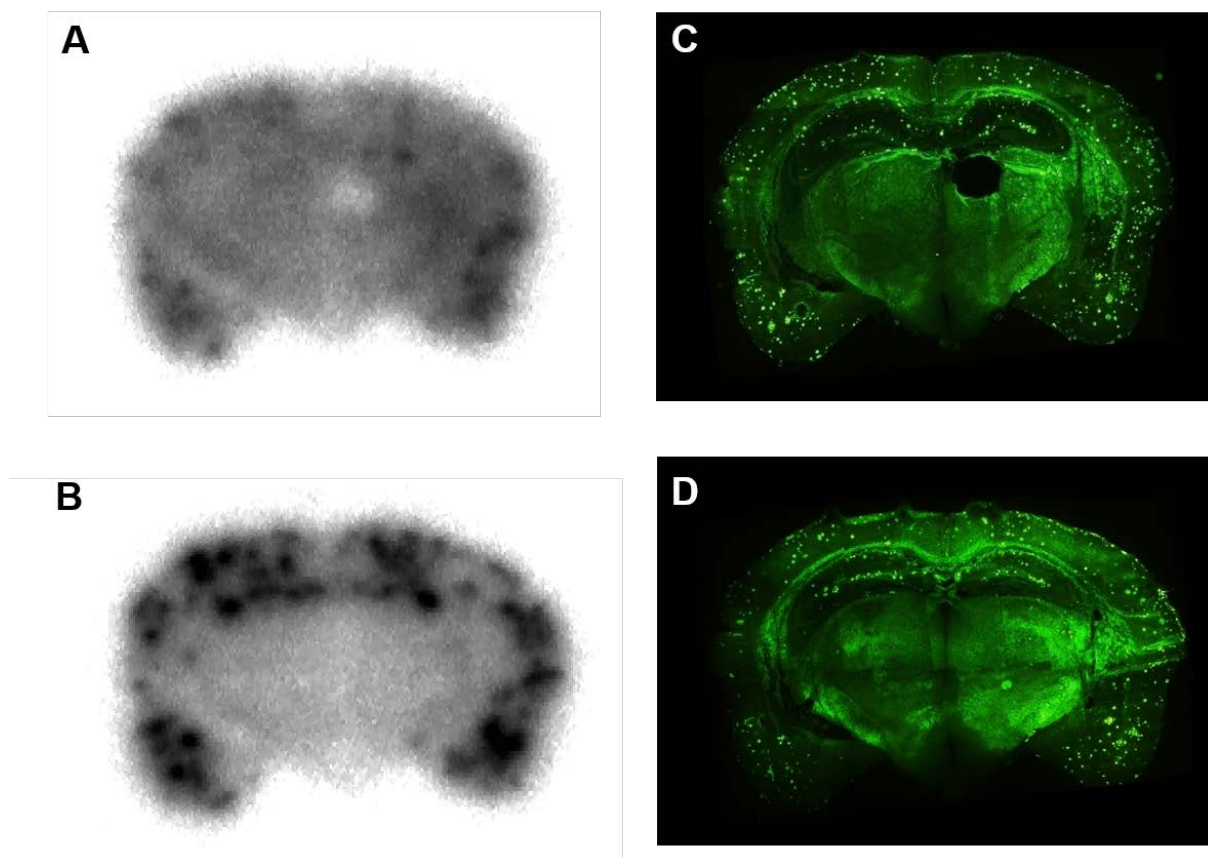age-matched control mouse brain sections. Scale bar= 50 μm.

Figure 3. *In vitro* autoradiograms of styrylchromone derivatives [^{125}I]**14** (A) and [^{125}I]**15** (B) in the brain sections of *Tg2576* mouse brain. Fluorescence images of thioflavin-S in the adjacent section (C and D).